Roles of PknB and CslA in cell wall morphogenesis of *Streptomyces*

Marta Derkacz[1], Andrew Watson[2], Akshada Gajbhiye[3], Michał Tracz[4], Dagmara Jakimowicz[1], Matthias Trost[3], Jeff Errington[2,5] and Bernhard Kepplinger[1,2*]

[1] University of Wroclaw, Department of Molecular Microbiology, ul. F. Joliot-Curie 14a, 50-383 Wrocław, PL

[2] University of Newcastle, Centre for Bacterial Cell Biology, Baddiley-Clark Building, Newcastle upon Tyne NE2 4AX, UK

[3] Newcastle University Biosciences Institute, Faculty of Medical Sciences, Newcastle upon Tyne, NE2 4HH, UK

[4] University of Wroclaw, Mass Spectrometry Laboratory, ul. F. Joliot-Curie 14a, 50-383 Wrocław, PL

[5] The University of Sydney, Faculty of Medicine and Health, Sydney, NSW 2006, AU

* Corresponding author: bernhard.kepplinger@uwr.edu.pl

Key words: DivIVA, PknB, CslA, Tip Organising Centre (TIPOC), polarisome, cell morphogenesis, cell wall, phosphorylation, *Streptomyces*

Abstract

The bacterial cell wall is essential for maintaining cellular integrity and defining the mode of growth, with different species adopting distinct strategies for cell wall synthesis and remodelling. *Streptomyces* are filamentous bacteria predominantly found in soil and renowned for producing specialised metabolites, including antibiotics. They grow through tip extension and branching hyphal filaments, forming a multicellular mycelium. New branches are established by forming a new growth zone on the lateral cell wall. Proteins involved in this process are organised into complexes called polarisomes, with DivIVA being the most well-characterised component. To investigate the tip growth requirements in *Streptomyces albus* we developed a genetic screen utilising toxic DivIVA overproduction and searched for suppressors of its lethality, reasoning that such suppressors would likely encode components functionally linked to DivIVA or the tip growth machinery. Among the identified genes was *pknB*, encoding a serine/threonine protein kinase implicated in the regulation of cell growth and morphogenesis. We confirmed that deletion of *pknB* restored the growth phenotype of *S. albus* following DivIVA overproduction. The phosphoproteome analysis revealed that the absence of PknB alters the phosphorylation state of CslA, a cellulose synthase-like protein. We demonstrate that a phosphoablative mutant of CslA impairs β-glucan synthesis and causes hypersensitivity to lysozyme. Overproduction of CslA restored colony growth defects arising from DivIVA-induced hyperbranching, without however suppressing the hyperbranching phenotype.

These findings collectively identify PknB-dependent phosphorylation of CslA as a central regulatory point in *Streptomyces* cell envelope construction, revealing how modulation of β-glucan synthesis can mitigate the cellular consequences of DivIVA dysregulation.

Introduction

Peptidoglycan, a major target for antibiotics, is an essential component of bacterial cell walls, providing structural integrity and rigidity and enabling bacteria to maintain their shape and withstand osmotic pressure challenges (Liu and Breukink, 2016; Garde *et al.*, 2021). Proteobacteria (e.g., *Escherichia coli*) and Firmicutes (e.g., *Bacillus subtilis*) are among the best-studied models for cell morphogenesis. These rod-shaped bacteria typically exhibit lateral insertion of new cell wall material during elongation (Egan *et al.*, 2020). In contrast, Actinobacteria (e.g., *Streptomyces* and *Mycobacteria*) mainly insert new cell wall material at the tips during exponential growth (Flärdh, 2003a; Kuru *et al.*, 2014; Zambri *et al.*, 2025). Actinobacteria can be unicellular, such as Mycobacteria or Corynebacteria, or multicellular (e.g., *Streptomyces*), the latter forming a complex mycelial network that supports substrate colonisation (Chater, 2006). This polar growth mode is hypothesised to confer ecological advantages, such as efficient nutrient foraging and competitive dominance in soil environments.

Cell wall biosynthetic proteins driving tip growth are organised locally into polarisome complexes (Hempel *et al.*, 2008). Within the polarisome, DivIVA—a coiled-coil protein—plays a pivotal role and is essential for *Streptomyces* growth (Flärdh, 2003b). Overproduction of DivIVA results in swollen tips and hyperbranching, likely due to the misregulation of the cell wall biosynthetic machinery (Flärdh, 2003b). New DivIVA complexes appear on the lateral wall preceding the formation of the new branches (Flärdh, 2003b; Hempel *et al.*, 2008; Richards *et al.*, 2012). Two additional scaffolding proteins, Scy and FilP, are believed to sequester DivIVA, thereby facilitating the establishment of new growth zones and influencing the size and position of DivIVA complexes, respectively (Holmes *et al.*, 2013; Fröjd and Flärdh, 2019). The precise mechanism for branch initiation remains however elusive (Hempel *et al.*, 2008).

DivIVA phosphorylation has been reported in a wide range of species (Kang *et al.*, 2005; Beilharz *et al.*, 2012; Elsholz *et al.*, 2012). *Streptomyces coelicolor* encodes at least 34 Ser/Thr kinases, and DivIVA is modified by the non-essential Ser/Thr kinase AfsK (Hempel *et al.*, 2012). Mass spectrometry has identified AfsK phosphorylation sites on DivIVA as occurring on the non-essential C-terminal protein at residues T304, S309, S338, S344, and S355 in *S. coelicolor* (Saalbach *et al.*, 2013).The phosphatase SppA appears to function as a counterpart in this process (Passot *et al.*, 2022). Notably, AfsK overexpression induces disassembly of the apical (mother)

73 polarisome, leading to the formation of multiple daughter polarisomes, followed by the
74 establishment of multiple hyphal branches (Hempel *et al.*, 2008).
75 In contrast, in Mycobacteria, the DivIVA homologue Wag31 is phosphorylated by the essential
76 kinases PknA and PknB (Jani *et al.*, 2010). These genes reside within the division and cell wall
77 gene cluster that encodes key components of the bacterial cell division and peptidoglycan
78 biosynthesis machinery (Molle and Kremer, 2010). It typically includes *fts* genes for Z-ring
79 assembly, *mur* genes for peptidoglycan precursor synthesis, *rod-pbpA* genes for the cell wall, and
80 regulatory serine/threonine kinases *pknA* and *pknB*. Interestingly, the elimination of the
81 homologous kinase PknB in *Streptomyces* has no detrimental effect, whereas the kinase PknA is
82 missing in most *Streptomyces spp.* (Jones *et al.*, 2011).
83 In this study, we investigated the consequences of DivIVA overproduction in *Streptomyces albus*
84 to uncover the factors that are involved tip growth. This study revealed that inactivation of the
85 kinase PknB unexpectedly alleviated defects resulting from DivIVA imbalance. Subsequent
86 analysis identified CslA as a key downstream target of PknB, a cellulose synthase–like protein that
87 synthesises β-glucan and contributes to cell wall biogenesis (Xu *et al.*, 2008). We further
88 demonstrate that CslA phosphorylation state modulates β-glucan- synthesis and, consequently, the
89 cell's ability to stabilise growth zones. These findings suggest a phosphorylation-dependent
90 regulatory mechanism linking PknB activity to cell wall assembly at hyphal tips.
91

92 # Materials and methods

93 **Bacterial strains and culture conditions**

94 All *S. albus* strains used in this study are listed in Table S1. *S. albus* spores were collected using
95 standard protocols (Kieser T *et al.*, 2000) from cultures grown on Soya Flour Mannitol (SFM) agar
96 plates supplemented with antibiotics (if required) to a final concentration of apramycin (50 µg/mL)
97 and hygromycin (50 µg/mL). Spore concentration was determined by serial dilution on SFM agar
98 plates. Spores were maintained at–80 °C in 25% glycerol aliquots for single-use. Tryptic Soy Broth
99 (TSB) and 5% TSB were used for morphology experiments. Liquid cultures were performed in 250
100 mL Erlenmeyer flasks containing metal spirals at 30 °C and 220 rpm for agitation. Solid cultures
101 were grown on 20 mL of 2% or 5% TSA agar plates at 30 °C. *E. coli* strains (listed in Table S2)
102 were grown at 37 °C on LB supplemented with antibiotics (if required) to a final concentration of

103 apramycin (50 µg/mL), kanamycin (50 µg/mL), chloramphenicol (34 µg/mL), or on 2YT
104 supplemented with hygromycin (50 µg/mL).

105 **Construction of plasmids and strains**

106 All plasmids and oligonucleotides used in this study are listed in Table S3 and Table S4,
107 respectively. Details of the plasmid construction are provided in the Supplementary Methods,
108 specifically in the section on comprehensive plasmid design and assembly. Plasmids were
109 transformed into *E. coli* DH5α and subsequently transferred to *Streptomyces* by conjugation with
110 *E. coli* ET12567/pUZ8002 strain or protoplast transformation using standard protocols (Kieser T
111 *et al.*, 2000). For integrative plasmids, *Streptomyces* strains were grown in the presence of the
112 appropriate antibiotics. CRISPR/Cas9 plasmids were cured by incubation at 42 °C without
113 antibiotics. Mutants lacking apramycin resistance were sequenced by Microsynth AG using PCR-
114 amplified fragments of modified genomic DNA (with the exception of the 65α, 65α attBϕC31::
115 pIJ6902 (empty plasmid), and 65α attBϕC31::pBK288 (CslA under *tipA* inducible promoter)
116 strains, which were verified by Illumina sequencing).

117 **Selection of spontaneous suppressor mutants and bioinformatics analysis**

118 Spores of the DivIVA overproduction strain (approximately 10^6 spores per plate) were spread onto
119 5% TSA plates supplemented with 500 ng/mL of inducer (anhydrotetracycline). Following 5 days
120 of incubation, several colonies were observed and subsequently restreaked onto fresh 5% TSA
121 containing 500 ng/mL of the inducer (anhydrotetracycline). The parent DivIVA-overproducing and
122 wild-type strains served as controls.

123 DNA was isolated from the strains using a modified version of the "salting-out" method (Pospiech
124 and Neumann, 1995; Watson *et al.*, 2022). Libraries for Illumina sequencing were prepared using
125 the Illumina DNA prep kit, Nextera XT kit, and Illumina Nextera XT primer Index Kit. Sequencing
126 was performed by Edinburgh Genomics using MiSeq v2 (250 PE). Raw sequences are available in
127 the NCBI Sequence Read Archive (accession number: PRJNA1099611).

128 The quality of all Illumina reads was assessed using fastQC (version 0.11.9), and the reads were
129 trimmed using trimmomatic (version 0.39). Bowtie2 (version 2.3.5.1) was used to align the
130 trimmed Illumina reads to the *Streptomyces albus* J1074 genome (NC_020990.1) using the very
131 sensitive preset mode for mapping paired-end reads. Variants were called using bcftools (version
132 1.14) in the consensus calling mode (-c). Only predicted variants with a QUAL score of ≥ 15 were
133 retained. Bedtools subtract (version 2.27.1) was used to filter out any variants identified in potential

134 suppressor strains that were already present in the lab *S. albus* J1074 parent strain compared to the
135 reference sequence (NC_020990.1) and thus were accumulated independently from this
136 experiment. The potential impact of all variants on protein-coding sequences was assessed using
137 snpEff (version 5.0e) (Cingolani *et al.*, 2012). The final table was derived by manually inspecting
138 shortlisted mutations.

139 **Microscopy**

140 For phenotypic analysis, 10^7 colony-forming units (CFU) of *S. albus* J1074 strains were inoculated
141 into 20 mL TSB or 5% TSB, with or without 250 ng/mL anhydrotetracycline (ATc), and cultured
142 for 20 h.

143 For β-glucan staining, $2 \cdot 10^6$ CFU (estimated by OD_{600} measurement) of *S. albus* J1074 strains from
144 freshly grown SFM agar plates were inoculated in 20 ml TSB and cultured for 20 h. Cells were
145 centrifuged and washed with modified PEM buffer (0.4 M PIPES, 20 mM EDTA, 20 mM $MgCl_2$;
146 pH = 6.9 (KOH)), stained with lectin dye (Sigma-Aldrich L3892) for 5 min at room temperature,
147 washed, and resuspended in modified PEM buffer (Hasek, 2006).

148 Cells were centrifuged as needed, loaded onto a 1.2% agarose slide prior to imaging, and examined
149 using a Leica DM6 B fluorescence microscope equipped with a 100× objective and a DFC7000
150 GT camera. Images were analysed using the ImageJ software.

151 To determine the β-glucan content (Fig. 3), the mean fluorescence signal was measured at each tip
152 (within a 20-pixel diameter circle). A minimum of 574 data points were collected for each strain
153 tested. Data were analysed and visualised using R software, including the ggplot2 package
154 (Ehrlinger, 2016). Statistical analysis was performed using analysis of variance (ANOVA),
155 followed by Tukey's HSD post-hoc test.

156 **Protein extraction for mass spectrometry**

157 For mass spectrometry, 10^7 CFU of WT or Δ*pknB* were inoculated in 50 mL of TSB or 5% TSB
158 and cultured for 20 h. Four biological replicates were performed under each condition. Mycelia
159 were harvested by centrifugation (5 min, 4 °C, 3000 × g), washed twice with phosphate-buffered
160 saline (PBS), and resuspended in 8 M urea buffer supplemented with 50 mM Tris, 1 mM TCEP
161 (Roth), a protease inhibitor (Thermo Scientific), and a phosphatase inhibitor consisting of sodium
162 molybdate (115 mM), sodium orthovanadate (100 mM), sodium tartrate dihydrate (400 mM),
163 glycerophosphate (500 mM), and sodium fluoride (100 mM). Five millilitres of buffer was used
164 per gram of biomass. Cell disruption was achieved via sonication (2 × 20 s, 4 °C, 20 kHz), followed

165 by centrifugation (15 min, 4 °C, 3000 × g), and the resulting supernatant was stored at–80 °C prior
166 to subsequent steps. A detailed protocol for further sample preparation and instrumental analysis
167 is provided in the Supplementary Information.

168 **Lysozyme sensitivity and survival assays**

169 Sensitivity to lysozyme was assessed by inoculating 5 µL of PBS spore suspensions and 1:10
170 dilutions onto TSA plates supplemented with lysozyme at a final concentration of 25 µg/mL,
171 compared to a no-addition control (Fig. 3A). Cultures were incubated for 3 days. Survival assays
172 were performed similarly using TSA and 5% TSA, both supplemented or not with
173 anhydrotetracycline at 500 ng/mL. To determine whether osmotic stress conditions induced by 5%
174 TSA affected the lethality of the inducible DivIVA production strain (strain 65α), 0.5 M sucrose
175 was added to the 5% TSA.

176 **DivIVA-mScarlet production analysis**

177 For western blot analysis, 2×10^7 CFU of *Streptomyces* strains were inoculated in 50 mL of TSB
178 or 5% TSB, in the presence or absence of ATc (250 ng/mL), and cultured for 24 h. Up to 50 mL of
179 cultured mycelia were harvested by centrifugation (5 min, 4 °C, 3000 × g), washed twice with PBS,
180 and resuspended in 1 mL PBS supplemented with a protease inhibitor (Thermo Fisher Scientific)
181 and 1 mM DTT. Cell disruption was achieved via sonication (2 × 20 s, 4 °C, 20 kHz), followed by
182 mixing with 6x loading buffer and denaturation (15 min, 95 °C). Total protein concentration was
183 normalised and assessed using SDS-PAGE containing 2.5% 2, 2, 2-trichloroethanol (Thermo
184 Scientific). Proteins were visualised using a stain-free filter on a ChemiDoc (Bio-Rad). Signal
185 intensity was measured using ImageJ software, and the samples were adjusted accordingly.
186 Proteins were transferred to a nitrocellulose membrane, which was blocked with a blocking
187 solution (5% powdered milk in PBST [PBS with 0.1% Tween-20]), then incubated with either
188 rabbit anti-mCherry polyclonal antibody (diluted 1:1000 in fresh blocking solution) or anti-
189 $DivIVA_{SC}$ antiserum (diluted 1:5000 (gift from Prof, Klas Flärdh, Lund University) (Wang *et al.*,
190 2009). The membrane was washed thrice with PBST and incubated with goat anti-rabbit IgG cross-
191 linked to horseradish peroxidase (Santa Cruz Biotechnology; diluted 1:5000 in fresh blocking
192 solution), followed by three washes with PBST. The blot was incubated with SuperSignal ™ West
193 Pico PLUS Chemiluminescence Substrate (ThermoScientific) and visualised using a ChemiDoc
194 (BioRad).
195

196 **Growth Assay with Induced *cslA* Mutant**

197 Overnight cultures were harvested by centrifugation and washed thrice with phosphate-buffered
198 saline (PBS). The optical density (OD) of the washed cells was adjusted to 0.1, and aliquots were
199 plated onto 5% tryptic soy agar (TSA) plates supplemented with either 500 ng/mL of the DivIVA
200 inducer and/or 0.5 µg/mL of thiostrepton.

201

202 # Results

203 **Identification of conditions for lethality of a DivIVA overexpression construct**

204 The scaffolding protein DivIVA is localised at the tip of the *Streptomyces* hyphae and is essential
205 for regulating normal apical growth (Flärdh, 2003b; Hempel *et al.*, 2008). Previous studies have
206 demonstrated that overproduction of DivIVA leads to hyphal tip swelling and overbranching
207 (Hempel *et al.*, 2008). We hypothesised that lethal overproduction of DivIVA could be suppressed
208 by mutations in genes encoding proteins involved in tip growth and cell wall remodelling. Initially,
209 we constructed a strain carrying a *divIVA-mScarlet* fusion under the control of an
210 anhydrotetracycline (ATc)-inducible promoter located in the phiBT1 locus. Although induction of
211 this fusion protein was non-lethal, during the development of additional derivatives, we
212 serendipitously created a strain, designated 65α, harbouring two inducible copies of *divIVA-*
213 *mScarlet*, one in the native locus and the other at the phiBT1 locus (Fig. 1A). This strain was able
214 to grow in the absence of the inducer, presumably because of leaky expression from the promoter
215 (Fig. 1B). However, upon induction, a strong fluorescence signal was observed at the hyphal tips,
216 accompanied by swelling and hyperbranching (Fig. 1C), aligning with previously documented
217 observations from a DivIVA overproduction strain of *S. coelicolor* (Flärdh, 2003b; Hempel *et al.*,
218 2008). After testing a range of growth conditions, we found that under hypoosmotic stress
219 conditions (1/20 reduced concentration of TSA medium "5% TSA"), the growth of strain 65α was
220 abolished in the presence of the inducer, while it grew similarly to the wild type in its absence (Fig.
221 1B), suggesting cell wall damage leading to osmotic lysis (rescued by 0.5 M sucrose; Fig. S1).

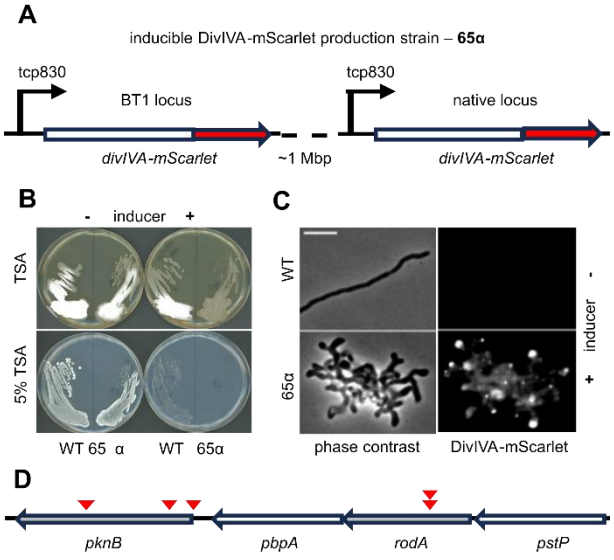

Figure 1 Genetic configuration and phenotype of DivIVA overproducing strain 65α (A) Pictorial representation of the genetic makeup of the *S. albus* J1074 mutant, called 65α, containing two copies of a *divIVA-mScarlet* fusion under the control of the ATc inducible promoter tcp830. (B) Comparison of the growth behaviour of the wild-type *S. albus* J1074 and the inducible mutant strain 65α on TSA and 5% TSA in the presence or absence of the inducer (500 ng/mL). (C) Microscopic phenotypes of *S. albus* J1074 wild-type strain and 65α mutant grown in TSB in the presence of the inducer (250 ng/mL). Fluorescent phase-contrast microscopy demonstrated DivIVA-mScarlet localisation. Scale bar - 5 µm. (D) Genetic organisation of the gene cluster containing *pknB* and *rodA* in *S. albus* J1074 (3,450,591-3,457,165 on NC_020990; ~1Mbp from BT1 locus and ~2Mbp from *divIVA* locus). The red arrows indicate the locations of the mutations described in Table 1.

Table 1: Genes recurrently mutated across independent suppressor mutants

Gene Name	*Protein names*	*Mutant number* [a]	*Amino acid change* [b]
XNR_RS08380	prolyl serine peptidase	2	M34:P63fs; M43:P63fs
XNR_RS15060	PknB	3	M25: M1fs; M40: A396D; M43: S98fs
XNR_RS15070	RodA	2	M33: L162del; M34: L162del

[a] Mutant number refers to the frequency at which a mutation in a gene was recovered in a different mutant strain. The amino acid change indicates the result of a mutation in the corresponding mutant strain starting with M.
[b] fs – frame shift; del – deletion

246 **A suppressor screen for mutations bypassing *divIVA* overexpression lethality**

247 To identify genes potentially influencing hyphal growth, we plated *divIVA* overexpression strain
248 65α under the lethal conditions described above and picked the rare colonies that emerged. Of the
249 43 colonies from three different starting cultures, 13 mutant strains displayed robust growth under
250 65α lethal conditions.

251 Because we had two separate copies of the *divIVA* construct, we expected the suppressor mutations
252 to lie in genes other than *divIVA*. Whole-genome sequencing followed by bioinformatic analysis
253 of the 13 mutants revealed apparent mutations in 122 coding regions (File S1). Table 1 lists the
254 genes in which more than one mutation was identified. Of these, XNR_RS15060 and
255 XNR_RS15070 were particularly interesting. They are located almost adjacent to each other in the
256 division and cell wall (DCW) cluster, and their identities are apparent from the conservation of the
257 gene cluster relative to other actinobacteria. We annotated these as *pknB* (XNR_RS15060) and
258 *rodA* (XNR_RS15070) based on their homology to the equivalent operon in *S. coelicolor* (Fig.
259 1D). In *pknB*, we identified two distinct frameshift mutations: one affecting the start codon and the
260 other located within the kinase domain near the N-terminus. An additional variant of this gene
261 consisted of a single nucleotide substitution within the PASTA domain (Fig. S2).

262 PknB kinase is an essential protein in *Mycobacterium tuberculosis* (Chawla *et al.*, 2014) and
263 *Corynebacterium glutamicum* (Fiuza *et al.*, 2008), and conditional *pknB* mutations affect the
264 maintenance of cell shape (Arora *et al.*, 2018). PknB also phosphorylates DivIVA in Mycobacteria,
265 but not in *Streptomyces* (Kang *et al.*, 2005; Hempel *et al.*, 2012). The exact role of PknB in
266 *Streptomyces* has not been elucidated, as deletion of *pknB*, in contrast to other bacteria, has no
267 deleterious effect, at least in wild-type cells (Jones *et al.*, 2011). The network of interactions
268 described above, involving various proteins involved in cell morphogenesis, prompted us to focus
269 on the role of PknB.

270

271 **Deletion of *pknB* rescues *Streptomyces* from lethal overexpression of *divIVA***

272 To test whether the mutations identified above were responsible for the suppression of the *divIVA*
273 overexpression phenotype, we attempted to delete *pknB* in wild-type and *divIVA* overexpression
274 (65α) strains. As expected, deletion of *pknB* did not result in any evident phenotypes in the wild-
275 type *S. albus* strain, consistent with previously reported results (Jones *et al.*, 2011). However, the

276 65α background deletion of *pknB* enabled growth under otherwise lethal conditions (5% TSA +
277 ATc) (Fig. 2A).
278 Microscopic imaging (Fig. 2B-C, quantification Fig. S3) revealed that the 65α strain had an
279 increased frequency of branching compared with the wild type, even in the absence of the inducer,
280 while in the presence of ATc, it exhibited hyperbranching, bulging, and an accumulation of
281 mScarlet at the hyphal tips. In contrast, the 65α Δ*pknB* strain exhibited reduced branching and a
282 diminished fluorescent signal compared with the 65α parent. Indeed, 65α Δ*pknB* mycelia closely
283 resembled those of the wild-type strain, even in the presence of ATc. Although we could still detect
284 a fluorescent signal from mScarlet, the fluorescence was notably reduced compared to that of 65α.
285 In the absence of the inducer, most hyphae (67%) exhibited a diffuse cytoplasmic distribution of
286 the mScarlet signal. Upon induction, this proportion decreased to approximately 33%, with the
287 remaining hyphae displaying a clear accumulation of fluorescence at the tips of the hyphae.
288 Sanger sequencing of both *divIVA-mScarlet* fusion genes did not reveal any mutations. Presumably,
289 the lowered signal at the hyphal tips could be a result of DivIVA-mScarlet being distributed more
290 widely throughout the hyphae or diminished protein levels due to decreased synthesis or increased
291 degradation.
292 To compare the total DivIVA protein levels between strains, we analysed DivIVA–mScarlet
293 abundance in 65α and 65α *ΔpknB* by Western blotting using anti-mScarlet- and anti-
294 DivIVA- antibodies (Fig. 2D; loading control in Fig. S4). Native DivIVA (predicted 41.1 kDa)
295 migrated at approximately 60 kDa in both wild-type and Δ*pknB* backgrounds. Its abundance was
296 not significantly altered in the absence of *pknB*. The upward shift in the apparent molecular weight
297 likely reflects dimerisation or altered electrophoretic mobility. In the 65α background, the
298 DivIVA–mScarlet fusion protein (predicted 68 kDa) migrated near 100 kDa. Upon ATc induction,
299 the intensity of the full-length fusion increased strongly when detected by both the anti-DivIVA
300 and anti-mScarlet antibodies, confirming that induction elevated total DivIVA–mScarlet levels.
301 Both *65α* and *65α ΔpknB* strains displayed additional faster-migrating- species. These fragments
302 were detected by anti-DivIVA but not by anti-mScarlet antibody, indicating that they represent N-
303 terminal- DivIVA cleavage products lacking the fluorescent tag. Conversely, the anti-
304 mScarlet- blot revealed smaller mScarlet-containing- fragments not recognised by anti-DivIVA-,
305 consistent with C-terminal- cleavage events. ATc induction increased the abundance of these
306 fragments in *65α*, consistent with the higher overall expression of the fusion protein.

307 Loss of *pknB* did not reduce the amount of full-length- DivIVA–mScarlet; however, it markedly
308 altered the pattern of degradation products. The 65α *ΔpknB* strain accumulated several distinct
309 DivIVA-sized fragments, suggesting that *pknB* influences the stability or processing of the
310 DivIVA–mScarlet fusion protein indirectly. This raises the possibility that PknB-dependent
311 signalling influences the proteolytic turnover of DivIVA, potentially serving as a mechanism to
312 control DivIVA levels under conditions of overexpression.

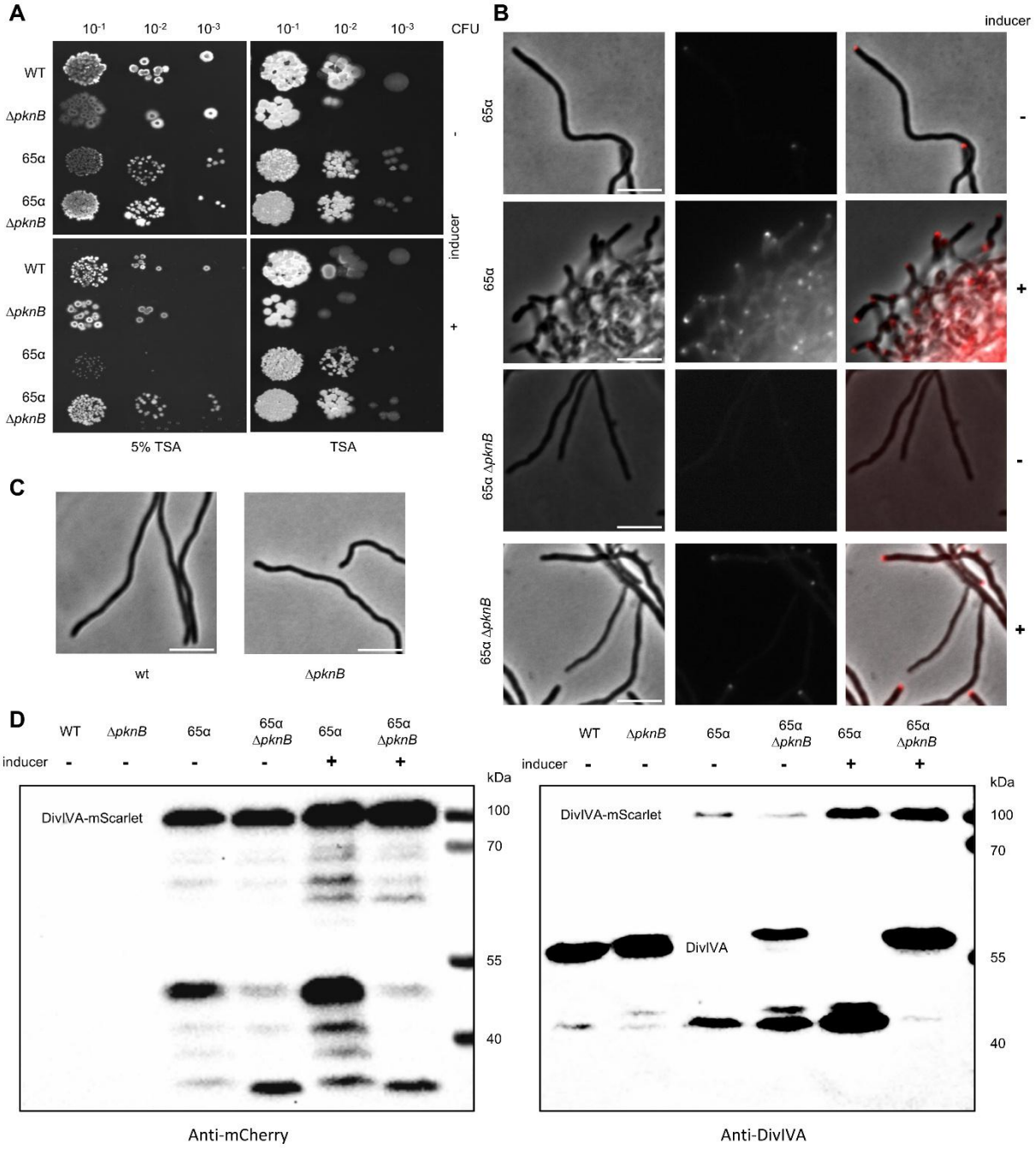

Figure 2 Verification of *pknB* deletion as a suppressor of lethal DivIVA overproduction. (A) Survival assay of *S. albus* J1074 strains grown on 5% TSA or TSA in the presence or absence of the inducer - ATc 500 ng/ml. B) Phenotypes of *S. albus* J1074 strains grown in TSB in the presence or absence of the inducer ATc (100 ng ml^{-1}). Fluorescence and phase-contrast microscopy revealed DivIVA–mScarlet production. Fluorescence backgrounds and intensity thresholds were adjusted identically across samples to allow for direct comparison. In the overlay panel, fluorescence levels were adjusted for improved visualisation. Scale bar, 5 µm. (C) Phase-contrast microscopy of *S. albus* J1074 and *S. albus* J1074 Δ*pknB* grown in TSB. (D)Western blot analysis of DivIVA-mScarlet (theoretical mass ~68 kDa) production by *S. albus* J1074 strains grown in TSB, in the presence or absence of the inducer - ATc 250 ng/ml. Left Detection was performed using anti-mCherry polyclonal antiserum. Right Detection was performed using anti-$DivIVA_{SC}$ antiserum. The molecular weight (MW) values to the right indicate the positions of the marker proteins.

324 **Deletion of *pknB* causes hyperphosphorylation of CslA**

325 The kinase PknB has been reported to be involved in various processes across various organisms,
326 including cell division, peptidoglycan synthesis, protein synthesis, and stress responses (Jones *et*
327 *al.*, 2011; Dworkin, 2015; Richard-Greenblatt and Av-Gay, 2017). To better understand its role in
328 *S. albus,* we analysed the phosphoproteomes of wild-type and Δ*pknB S. albus* strains, with
329 particular focus on proteins implicated in polar growth. The results identified 27 phosphorylated
330 proteins, of which three were significantly hypophosphorylated in the *pknB* mutant, while one was
331 significantly hyperphosphorylated (
332 Table 2 and File S2; proteomics data are available in File S3). Among the expected candidates, we
333 anticipated changes in DivIVA phosphorylation, as well as in other regulators such as the kinase
334 AfsK or the phosphatase SppA, which is known to dephosphorylate DivIVA (Hempel *et al.*, 2012;
335 Passot *et al.*, 2022). Although SppA phosphorylation was indeed altered in the Δ*pknB* background,
336 no corresponding changes in DivIVA phosphorylation were detected in our experimental setup,
337 and this pathway was therefore not investigated further. Our attention was drawn to CslA, a
338 synthase previously associated with polar growth, whose phosphorylation was
339 hyperphosphorylated on residue T17 in the Δ*pknB* background, making it a compelling candidate
340 for mediating PknB's effects on hyphal development. This protein localises at hyphal tips and is
341 responsible for the production of a beta-glucan-containing polysaccharide that is thought to provide
342 additional physical protection, potentially required for the continuous remodelling of the growing
343 cell wall (Xu *et al.*, 2008). Loss of this polymer impairs the morphological development and
344 stability of the cell wall (Xu *et al.*, 2008; Zhong *et al.*, 2022). CslA forms a protein complex with
345 the copper radical oxidase GlxA, and it is a known interaction partner of DivIVA in *S. coelicolor*
346 (Xu *et al.*, 2008).

347 To evaluate the effect of phosphorylation on the function of CslA, we constructed a strain
348 producing phosphoablative CslA ($cslA_{T17A}$) and a deletion mutant. We confirmed the production
349 of the phosphoablative ClsA using a proteomics experiment (Fig S5). Previous studies have shown
350 that deletion of *cslA* increases sensitivity to lysozyme (Zhong *et al.*, 2022); we therefore tested
351 whether preventing phosphorylation at T17 would similarly affect cell wall integrity. Both *cslA*
352 mutants displayed hypersensitivity to lysozyme, suggesting that phosphorylation is important for
353 CslA activity (Fig. 3A). To determine whether the reciprocal change — hyperphosphorylation of
354 CslA in the Δ*pknB* background — had the opposite effect, we assessed lysozyme sensitivity of the

355 *pknB* deletion strain. This strain responded to lysozyme similarly to the wild type, indicating that
356 hyperphosphorylation of CslA alone is not sufficient to further enhance cell wall protection beyond
357 wild-type levels. Next, we used a lectin dye to stain β-glucans (Fig. 3B-C) and found that the signal
358 at the tips of hyphae was completely abolished in the *cslA* knockout strain, similar to previously
359 reported data on a *cslA* deletion strain (Xu *et al.*, 2008; Zhong *et al.*, 2022). Again, the strain
360 producing phosphoablative variant of CslA (*cslA*$_{(T17A)}$) behaved similarly to the deletion strain
361 when stained for β-glucans, indicating that phosphorylation is likely required for the β-glucan
362 synthetic activity of CslA. Overall, these data indicate that phosphorylation plays an important role
363 in β-glucan production, although the role of PknB in this process is likely to be indirect.
364

365 Table 2 Significantly different protein phosphorylation patterns of *S. albus* J1074 WT and Δ*pknB* strains grown in TSB
366 medium.

locus_tag	protein name	phosphorylation in Δ*pknB* vs WT
XNR_RS17030	FolK	Hypophosphorylated ↓
XNR_RS11880	GroL	Hypophosphorylated ↓
XNR_RS08650	CslA	Hyperphosphorylated ↑
XNR_RS14580	SppA	Hypophosphorylated ↓

367

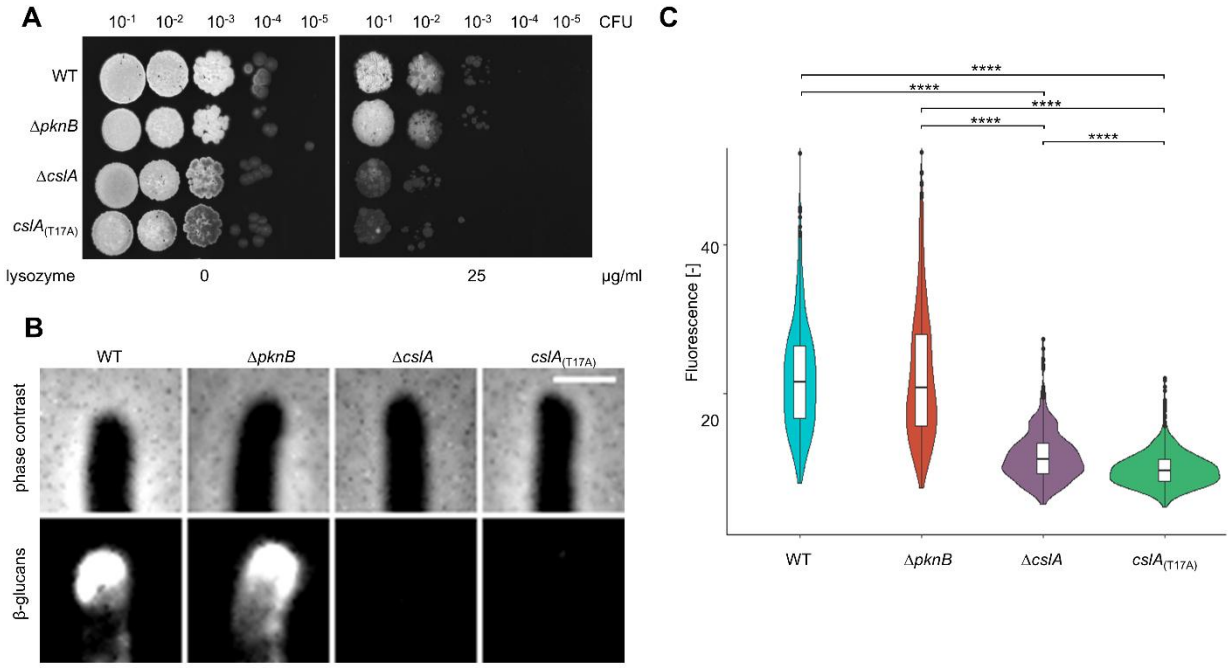

368

369 Figure 3 Figure 3 Impact of mutations in *cslA* on glucan production (A) Lysozyme sensitivity of *S. albus* J1074 strains
370 grown on TSA. (B) Phenotypes of *S. albus* J1074 strains grown on TSA. Cells were stained with lectin dye to visualise
371 β-glucans. Scale bar - 1 µm. (C) Quantification of mean β-glucan production at the tip by *S. albus* J1074 strains grown

372 in TSB. The width of each plot indicates the number of collected data points for a specific fluorescence. Significant
373 differences, according to ANOVA followed by Tukey's HSD post-hoc test, are marked with **** (p≤0,0001).
374

375 **Overexpression of CslA rescues cells from DivIVA overproduction lethality**

376 The results described above, showing that phosphorylation of CslA is likely required for the β-
377 glucan synthetic activity, suggest that the deletion of *pknB* might increase the activity of CslA, via
378 increased phosphorylation albeit indirectly. If so, *cslA* overexpression might also rescue cells from
379 *divIVA-mScarlet* overexpression toxicity. To test this, a plasmid carrying a thiostrepton-inducible
380 copy of *cslA* was introduced into the 65α background, with an empty plasmid as a control. In the
381 absence of DivIVA overproduction, both strains grew well on 5% TSA. However, even without
382 induction, the strain with the *cslA* plasmid exhibited significantly improved colonial growth
383 compared to the empty-plasmid control, likely due to leaky expression from the *tipA* promoter (Fig.
384 4A) (Tong *et al.*, 2019). Unexpectedly, *cslA* induction did not restore the overbranching phenotype
385 associated with *divIVA* overexpression, indicating that increased CslA only partially suppressed
386 the DivIVA overexpression phenotype (Fig. 4B, quantification Fig. S3). Plausibly, its contribution
387 to viability may involve the enhancement of the protective layer at the cell tip.

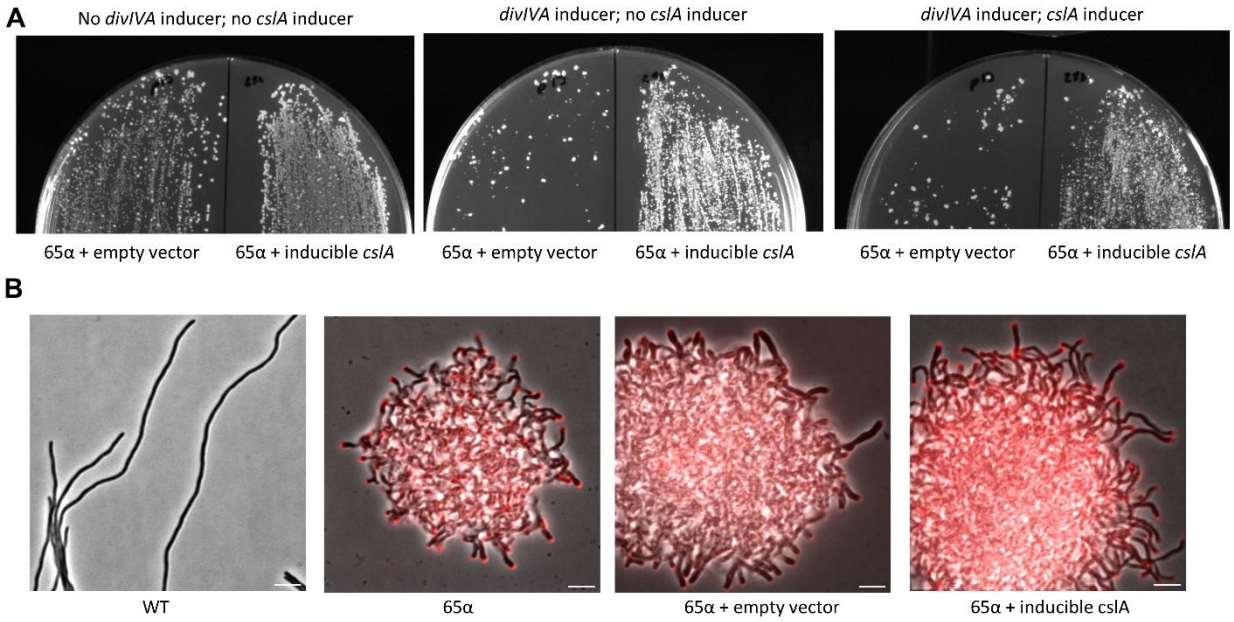

388
389 Figure 4 Overexpression of *cslA* rescues growth under conditions of DivIVA overproduction
390 (A) Growth of 65α attBϕC31::pIJ6902 (empty plasmid) and 65α attBϕC31::pBK288 (*cslA* under TipA inducible
391 promoter) grown on 5% TSB plates in the presence or absence of an inducer for DivIVA or CslA. (B) Phenotypes of
392 *S. albus* J1074 strains (WT, 65α, 65α attBϕC31::pIJ6902 [empty plasmid], and attBϕC31::pBK288 expressing *cslA*
393 under the TipA-inducible promoter) grown in 5% TSA medium in the presence of anhydrotetracycline (100 ng mL^{-1}).
394 DivIVA–mScarlet production was visualised by fluorescence microscopy and is shown as a red signal overlaid on
395 phase-contrast images. Fluorescence background and intensity thresholds were adjusted identically across all samples
396 to allow for direct comparison.

397

398 ## Discussion

399 To identify the factors required for tip growth and cell wall integrity, we performed a suppressor
400 screen based on the lethal overexpression of *divIVA*, a key polarity determinant. Under these
401 conditions, spontaneous suppressor mutants arise at low frequencies, and whole-
402 genome- sequencing revealed recurrent mutations in the Ser/Thr kinase gene *pknB*. PknB is a
403 conserved Ser/Thr kinase found across actinobacteria, where it has been implicated in the
404 regulation of cell division, cell wall synthesis, and stress responses. Targeted deletion of *pknB* in
405 the DivIVA overexpression background confirmed that the loss of this kinase is sufficient to
406 suppress lethality (Fig. 4), indicating that PknB activity becomes problematic when DivIVA-driven
407 tip formation is excessive.
408 Because PknB has been implicated in diverse cellular processes, we used global
409 phosphoproteomics to define its downstream targets. This analysis revealed that cellulose synthase
410 CslA was hyperphosphorylated in the absence of PknB. To determine the functional relevance of
411 this modification, we generated both a *cslA* deletion mutant and a phosphoablative T17A variant.
412 Substitution of T17 with alanine abolished CslA activity, as shown by quantitative microscopy and
413 increased lysozyme sensitivity, demonstrating that phosphorylation at this residue is essential for
414 its proper function. Conversely, *cslA* overexpression partially rescued the growth defect of the
415 DivIVA overproduction strain. However, ectopic overexpression of *cslA* did not restore normal
416 growth and the overbranching was still detected. Therefore, additional PknB-dependent targets
417 must contribute to the altered physiology observed in Δ*pknB* mutants. However, these findings
418 indicate that CslA is necessary for maintaining cell wall integrity of overbranching hyphae.
419 These findings identify PknB as a central regulator of cell wall homeostasis that becomes essential
420 when tip formation is elevated by DivIVA overproduction (Fig. 4). Furthermore, they implicate
421 CslA phosphorylation as a key downstream mechanism required to maintain cell wall integrity
422 under these conditions. The observation that CslA is more phosphorylated in the *pknB* mutant
423 suggests that PknB modifies activity of enzyme(s) that control phosphorylation of CslA. One
424 plausible model is that PknB represses a phosphatase or activates a second kinase, such that an
425 alternative kinase hyperphosphorylates CslA in the absence of PknB. In *Streptomyces*, several
426 Ser/Thr kinases, including AfsK, and the phosphatase SppA have established roles in controlling

427 cell polarity and cell wall–associated substrates, including DivIVA. Interestingly, SppA was
428 hypophosphorylated in our global phosphoproteome. Since SppA is known to dephosphorylate its
429 reduced phosphorylation in the Δ*pknB* background might be expected to result in altered DivIVA
430 phosphorylation DivIVA (Passot *et al.*, 2022). However, no corresponding changes in DivIVA
431 phosphorylation were detected in our experimental setup, suggesting that this pathway does not
432 play a major role under the conditions tested, or that compensatory mechanisms maintain DivIVA
433 phosphorylation levels. Whether SppA or another as-yet-unidentified enzyme mediates CslA
434 phosphorylation downstream of PknB remains to be determined. Thus, PknB likely acts upstream
435 of a broader regulatory network.
436 Finally, the DivIVA overexpression phenotype provides a physiological context for the observed
437 regulatory circuit. Excess DivIVA generates numerous closely spaced tips, creating multiple
438 mechanically vulnerable sites that require rapid reinforcement. The severe growth defect and
439 pronounced low osmolarity- sensitivity of the DivIVA overproduction strain are consistent with a
440 weakened cell envelope that is unable to withstand turgor pressure when tip reinforcement is
441 insufficient. In this scenario, CslA becomes particularly important, and its higher levels and correct
442 phosphorylation of CslA are likely required to deposit cellulose-rich material at all nascent growth
443 zones. The partial suppression of the DivIVA overexpression phenotype by *cslA* overexpression
444 fits naturally within this model; however, the failure of CslA overexpression to restore normal
445 growth in the Δ*pknB* background indicates that multiple PknB-dependent pathways are required to
446 maintain cell wall homeostasis when the tip number is increased.
447 In summary, using *divIVA* overexpression as a perturbation of tip-associated cell wall synthesis
448 allowed us to identify PknB as a central regulator of cell wall homeostasis, acting through a
449 phosphorylation network that ultimately controls CslA-dependent reinforcement of newly formed
450 tips, but also involving additional PknB-regulated factors that remain to be identified.

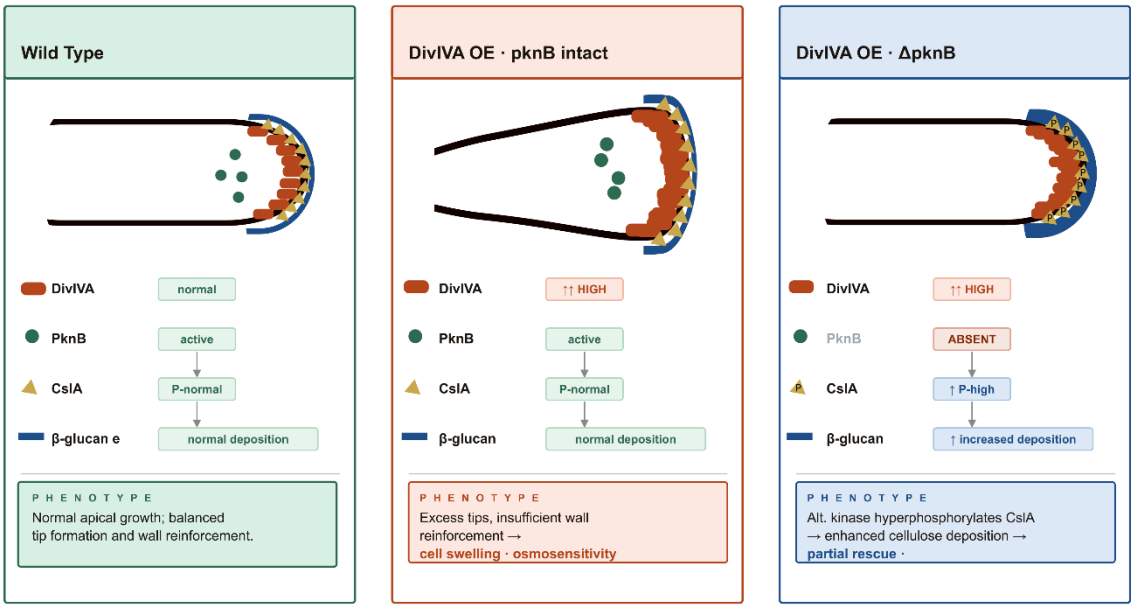

Figure 4 Proposed model of how phosphorylation regulates cell wall stability in *Streptomyces*, including the proposed roles of the kinase PknB and the cellulose-like synthase CslA.

Author contributions

Conceptualisation (B.K., J.E.), Funding Acquisition (B.K., J.E.), Investigation (M.D., B.K, A.W., A.G., M.T.), Project administration (B.K.), Supervision (B.K., M.T., J.E.), Visualization (B.K., M.D.), Writing – original draft (M.D., B.K.,). writing – review and editing (B.K., D.J., J.E.)

Acknowledgments

This work was funded by the Polish National Science Centre: Sonata grant 2020/39/D/NZ1/00303 to B.K. and a Wellcome Trust Investigator grant (209500) to JE.

We further wish to express our gratitude to Dr. Xiaobo Zhong (Leiden University) for useful discussions and advice regarding β-glucan staining.

We are grateful to Prof. Klas Flärdh (Lund University) for generously providing the DivIVA antiserum.

The purchase of M-Class Acquity-Synapt XS LC-MS system was financially supported by the "Excellence Initiative – Research University" program for the University of Wroclaw.

Data availability

The genome sequencing data that support the findings of this study are openly available in NCBI at https://www.ncbi.nlm.nih.gov/sra (accession number PRJNA1099611).

The mass spectrometry proteomics data have been deposited to the ProteomeXchange Consortium via the PRIDE (Perez-Riverol *et al.*, 2022) partner repository with the dataset identifier PXD053764 and PXD071342

Reviewer access details

Project accession: PXD053764

Token: tfcX8J5LlKQ2

Project accession: PXD071342

Token: jD9RJzE8ausd

484 # References

485 Arora, D., Chawla, Y., Malakar, B., Singh, A., and Nandicoori, V.K. (2018) The transpeptidase
486 PbpA and noncanonical transglycosylase RodA of Mycobacterium tuberculosis play important
487 roles in regulating bacterial cell lengths. *J Biol Chem* **293**: 6497–6516
488 https://doi.org/10.1074/jbc.M117.811190.

489 Beilharz, K., Nováková, L., Fadda, D., Branny, P., Massidda, O., and Veening, J.-W. (2012)
490 Control of cell division in Streptococcus pneumoniae by the conserved Ser/Thr protein kinase StkP.
491 *Proceedings of the National Academy of Sciences* **109**: E905–E913
492 https://doi.org/10.1073/pnas.1119172109.

493 Chater, K.F. (2006) Streptomyces inside-out: a new perspective on the bacteria that provide us with
494 antibiotics. *Philosophical Transactions of the Royal Society B: Biological Sciences* **361**: 761–768
495 https://doi.org/10.1098/rstb.2005.1758.

496 Chawla, Y., Upadhyay, S., Khan, S., Nagarajan, S.N., Forti, F., and Nandicoori, V.K. (2014)
497 Protein kinase B (PknB) of Mycobacterium tuberculosis is essential for growth of the pathogen in
498 vitro as well as for survival within the host. *Journal of Biological Chemistry* **289**: 13858–13875
499 https://doi.org/10.1074/jbc.M114.563536.

500 Cingolani, P., Patel, V.M., Coon, M., Nguyen, T., Land, S.J., Ruden, D.M., and Lu, X. (2012)
501 Using Drosophila melanogaster as a Model for Genotoxic Chemical Mutational Studies with a New
502 Program, SnpSift. *Front Genet* **3**: 1–9 https://doi.org/10.3389/fgene.2012.00035.

503 Dworkin, J. (2015) Ser/Thr phosphorylation as a regulatory mechanism in bacteria. *Curr Opin*
504 *Microbiol* **24**: 47–52 https://doi.org/10.1016/j.mib.2015.01.005.

505 Egan, A.J.F., Errington, J., and Vollmer, W. (2020) Regulation of peptidoglycan synthesis and
506 remodelling. *Nature Reviews Microbiology 2020 18:8* **18**: 446–460
507 https://doi.org/10.1038/s41579-020-0366-3.

508 Ehrlinger, J. (2016) ggRandomForests: Exploring Random Forest Survival.
509 http://arxiv.org/abs/1612.08974.

510 Elsholz, A.K.W., Turgay, K., Michalik, S., Hessling, B., Gronau, K., Oertel, D., *et al.* (2012)
511 Global impact of protein arginine phosphorylation on the physiology of Bacillus subtilis.
512 *Proceedings of the National Academy of Sciences* **109**: 7451–7456
513 https://doi.org/10.1073/pnas.1117483109.

514 Fiuza, M., Canova, M.J., Zanella-Cléon, I., Becchi, M., Cozzone, A.J., Mateos, L.M., *et al.* (2008)
515 From the characterization of the four serine/threonine protein kinases (PknA/B/G/L) of
516 Corynebacterium glutamicum toward the role of PknA and PknB in cell division. *Journal of*
517 *Biological Chemistry* **283**: 18099–18112 https://doi.org/10.1074/jbc.M802615200.

518 Flärdh, K. (2003a) Growth polarity and cell division in Streptomyces. *Curr Opin Microbiol* **6**: 564–
519 571 https://doi.org/10.1016/j.mib.2003.10.011.

520 Flärdh, K. (2003b) Essential role of DivlVA in polar growth and morphogenesis in Streptomyces
521 coelicolor A3(2). *Mol Microbiol* **49**: 1523–1536 https://doi.org/10.1046/j.1365-
522 2958.2003.03660.x.

523 Fröjd, M.J., and Flärdh, K. (2019) Apical assemblies of intermediate filament-like protein FilP are
524 highly dynamic and affect polar growth determinant DivIVA in Streptomyces venezuelae. *Mol*
525 *Microbiol* **112**: 47–61 https://doi.org/10.1111/mmi.14253.

526 Garde, S., Chodisetti, P.K., and Reddy, M. (2021) Peptidoglycan: Structure, Synthesis, and
527 Regulation. *EcoSal Plus* **9**: 1–35 https://doi.org/10.1128/ecosalplus.ESP-0010-2020.

528 Hasek, J. (2006) Yeast Fluorescence Microscopy. *Methods Mol Biol* **313**: 85–96
529 https://doi.org/10.1385/1-59259-958-3:085.

530 Hempel, A.M., Cantlay, S., Molle, V., Wang, S.B., Naldrett, M.J., Parker, J.L., *et al.* (2012) The
531 Ser/Thr protein kinase AfsK regulates polar growth and hyphal branching in the filamentous
532 bacteria Streptomyces. *Proc Natl Acad Sci U S A* **109**: E2371–E2379
533 https://doi.org/10.1073/pnas.1207409109.

534 Hempel, A.M., Wang, S., Letek, M., Gil, J.A., and Flärdh, K. (2008) Assemblies of DivIVA Mark
535 Sites for Hyphal Branching and Can Establish New Zones of Cell Wall Growth in Streptomyces
536 coelicolor. *J Bacteriol* **190**: 7579–7583 https://doi.org/10.1128/JB.00839-08.

537 Holmes, N.A., Walshaw, J., Leggett, R.M., Thibessard, A., Dalton, K.A., Gillespie, M.D., *et al.*
538 (2013) Coiled-coil protein Scy is a key component of a multiprotein assembly controlling polarized
539 growth in Streptomyces. *Proc Natl Acad Sci U S A* **110**: E397-406
540 https://doi.org/10.1073/pnas.1210657110.

541 Jani, C., Eoh, H., Lee, J.J., Hamasha, K., Sahana, M.B., Han, J.S., *et al.* (2010) Regulation of polar
542 peptidoglycan biosynthesis by Wag31 phosphorylation in mycobacteria. *BMC Microbiol* **10**: 327–
543 337 https://doi.org/10.1186/1471-2180-10-327.

544 Jones, G., Sol, R. Del, Dudley, E., and Dyson, P. (2011) Forkhead-associated proteins genetically
545 linked to the serine/threonine kinase PknB regulate carbon flux towards antibiotic biosynthesis in
546 Streptomyces coelicolor. *Microb Biotechnol* **4**: 263–274 https://doi.org/10.1111/j.1751-
547 7915.2010.00237.x.

548 Kang, C.M., Abbott, D.W., Sang, T.P., Dascher, C.C., Cantley, L.C., and Husson, R.N. (2005) The
549 Mycobacterium tuberculosis serine/threonine kinases PknA and PknB: substrate identification and
550 regulation of cell shape. *Genes Dev* **19**: 1692–1704 https://doi.org/10.1101/gad.1311105.

551 Kieser T, Bibb MJ, Buttner MJ, and Chater KF (2000) *Practical Streptomyces Genetics. 2nd ed.* .

552 Kuru, E., Tekkam, S., Hall, E., Brun, Y. V., and Nieuwenhze, M.S. Van (2014) Synthesis of
553 fluorescent D-amino acids (FDAAs) and their use for probing peptidoglycan synthesis and bacterial
554 growth in situ. *Nat Protoc* **10**: 33 https://doi.org/10.1038/nprot.2014.197.

555 Liu, Y., and Breukink, E. (2016) The Membrane Steps of Bacterial Cell Wall Synthesis as
556 Antibiotic Targets. *Antibiotics 2016, Vol 5, Page 28* **5**: 28
557 https://doi.org/10.3390/antibiotics5030028.

558 Molle, V., and Kremer, L. (2010) Division and cell envelope regulation by Ser/Thr
559 phosphorylation: Mycobacterium shows the way. *Mol Microbiol* **75**: 1064–1077
560 https://doi.org/10.1111/j.1365-2958.2009.07041.x.

561 Passot, F.M., Cantlay, S., and Flärdh, K. (2022) Protein phosphatase SppA regulates apical growth
562 and dephosphorylates cell polarity determinant DivIVA in Streptomyces coelicolor. *Mol Microbiol*
563 **117**: 411–428 https://doi.org/10.1111/mmi.14856.

564 Perez-Riverol, Y., Bai, J., Bandla, C., García-Seisdedos, D., Hewapathirana, S., Kamatchinathan,
565 S., *et al.* (2022) The PRIDE database resources in 2022: a hub for mass spectrometry-based
566 proteomics evidences. *Nucleic Acids Res* **50**: D543–D552 https://doi.org/10.1093/nar/gkab1038.

567 Pospiech, A., and Neumann, B. (1995) A versatile quick-prep of genomic DNA from gram-positive
568 bacteria. *Trends Genet* **11**: 217–218 https://doi.org/10.1016/s0168-9525(00)89052-6.

569 Richard-Greenblatt, M., and Av-Gay, Y. (2017) Epigenetic Phosphorylation Control of
570 Mycobacterium tuberculosis Infection and Persistence. *Microbiol Spectr* **5**: 1–23
571 https://doi.org/10.1128/microbiolspec.tbtb2-0005-2015.

572 Richards, D.M., Hempel, A.M., Flärdh, K., Buttner, M.J., and Howard, M. (2012) Mechanistic
573 Basis of Branch-Site Selection in Filamentous Bacteria. *PLoS Comput Biol* **8**: 1–8
574 https://doi.org/10.1371/journal.pcbi.1002423.

575 Saalbach, G., Hempel, A.M., Vigouroux, M., Flärdh, K., Buttner, M.J., and Naldrett, M.J. (2013)
576 Determination of Phosphorylation Sites in the DivIVA Cytoskeletal Protein of Streptomyces
577 coelicolor by Targeted LC–MS/MS. *J Proteome Res* **12**: 4187–4192
578 https://doi.org/10.1021/pr400524d.

579 Tong, Y., Whitford, C.M., Robertsen, H.L., Blin, K., Jørgensen, T.S., Klitgaard, A.K., *et al.* (2019)
580 Highly efficient DSB-free base editing for streptomycetes with CRISPR-BEST. *Proc Natl Acad*
581 *Sci U S A* **116**: 20366–20375 https://doi.org/10.1073/pnas.1913493116.

582 Wang, S.B., Cantlay, S., Nordberg, N., Letek, M., Gil, J.A., and Flardh, K. (2009) Domains
583 involved in the in vivo function and oligomerization of apical growth determinant DivIVA in
584 Streptomyces coelicolor. *FEMS Microbiol Lett* **297**: 101–109 https://doi.org/10.1111/j.1574-
585 6968.2009.01678.x.

586 Watson, A.K., Kepplinger, B., Bakhiet, S.M., Mhmoud, N.A., Chapman, J., Allenby, N.E., *et al.*
587 (2022) Systematic whole-genome sequencing reveals an unexpected diversity among
588 actinomycetoma pathogens and provides insights into their antibacterial susceptibilities. *PLoS Negl*
589 *Trop Dis* **16**: 1–23 https://doi.org/10.1371/journal.pntd.00101288.

590 Xu, H., Chater, K.F., Deng, Z., and Tao, M. (2008) A cellulose synthase-like protein involved in
591 hyphal tip growth and morphological differentiation in streptomyces. *J Bacteriol* **190**: 4971–4978
592 https://doi.org/10.1128/jb.01849-07.

593 Zambri, M.P., Baglio, C.R., Irazoki, O., Jones, S.E., Garner, E.C., Cava, F., and Elliot, M.A. (2025)
594 Streptomyces uses both polar and dispersed cell wall synthesis during exploratory growth. *Nature*
595 *Microbiology 2025 10:9* **10**: 2245–2256 https://doi.org/10.1038/s41564-025-02080-x.

596 Zhong, X., Zhang, L., Wezel, G.P. van, Vijgenboom, E., and Claessen, D. (2022) Role for a Lytic
597 Polysaccharide Monooxygenase in Cell Wall Remodeling in Streptomyces coelicolor. *mBio* **13**: 1–
598 15 https://doi.org/10.1128/mbio.00456-22.

599

600